Mantle xenoliths from Zapolyarnayay pipe comparison to Novinka pipe Upper Muna field Yakutia

Igor Ashchepkov, Alexander Ivanov, Nikolai Medvedev, and Nikolay Vladykin

- [1]Institute of Geology and Mineralogy SB RAS, Geology, Novosibirsk, Russian Federation (igor.ashchepkov@igm.nsc.ru)
- [2]Scientific research geological enterprise, ALROSA, Mirny, Russia
- [3]Nikolaev Institute of Inorganic Chemistry, Novosibirsk, Russia
- [4]A.P. Vinogradov Institute of Geochemistry SB RAS, Irkutsk, Russia

A. Photo of the open pit in the Zapolyarnaya pipe Upper Muna field.
B. Large gem quality diamond from Zapolyarnaya pipe.
C. D. diamonds from Zapolyarnaya pipe

A
.

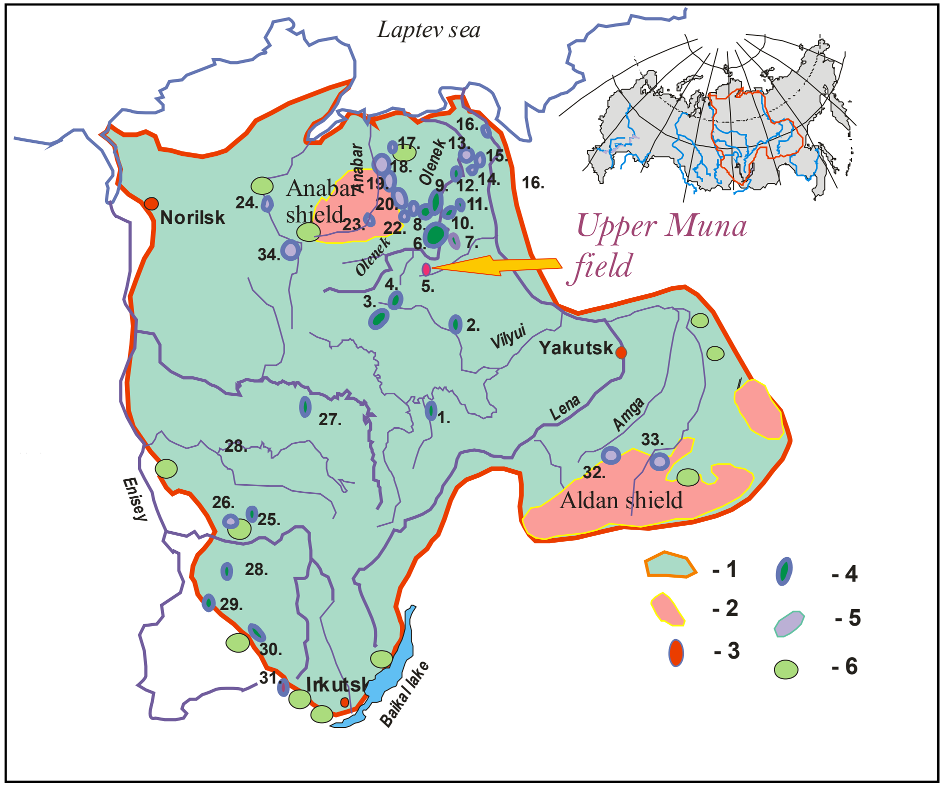

Fig.1. (A). Location of the Upper Muna field and otherkimberlite fields in Siberian platform

1.Siberian platform. 2 – Shields. Kimberlite fields: 3Upper Muna Field4. Late Devonian fields; 5. Lower Triassic and Jurassic fields (Kostrovitsky et al., 2007; Smelov et al., 2013). 6. Carbonatitic massifs . Fields: 1. Malo-Botuobinskoe, 2. Nakyn, 3. -Alakit-Markha, 4- Daldyn, 5 - Upper Muna, 6 — Chomurdakh, 7 - Severnei, 8 - West Ukukit, 9 - East Ukukit, 10 - Ust-Seligir, 11. Upper Motorchun, 12. Merchimden, 13. Kuoika, 14 - Upper Molodo, 15. Toluop, 16. Khorbusuonka, 17. Ebelyakh, 18. Staraya Rechka, 19. Ary-Mastakh, 20. Dyuken, 21. Luchakan, 22. Kuranakh, 23. Middle Kopnamka, 24. Middle Kotui, 25. Chadobets, 26. Taichikun-Nemba, 27. Tychan, 28. Muro-Kova, 29. Tumanshet, 30. Belaya Zima, 31. Ingashi, 32.- Chompolo, 33.Tobuk-Khatystyr, 34. Kharamai.

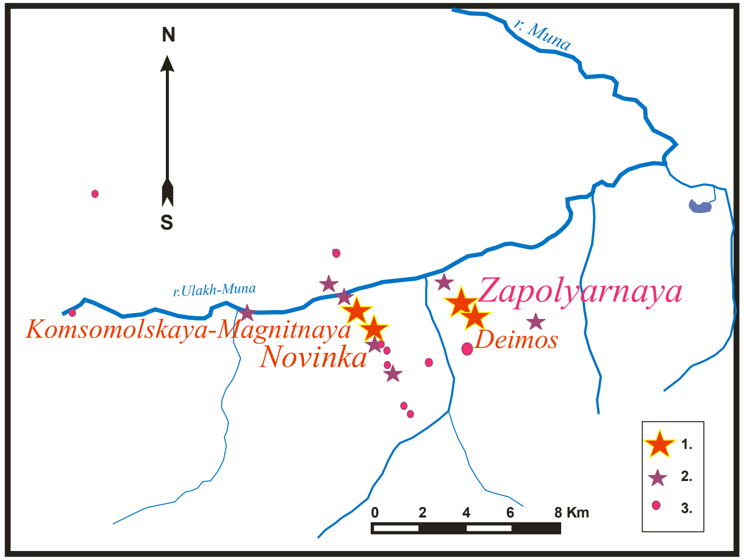

B
.

Scheme of the kimberlite pipes location in Upper Muna fiel

C.

Cross-sections from Upper Muna field to through Prianabarie to Lena Mouth according to thermobarometry of mantle xenocrysts

(Aschepkov et al, 2014)

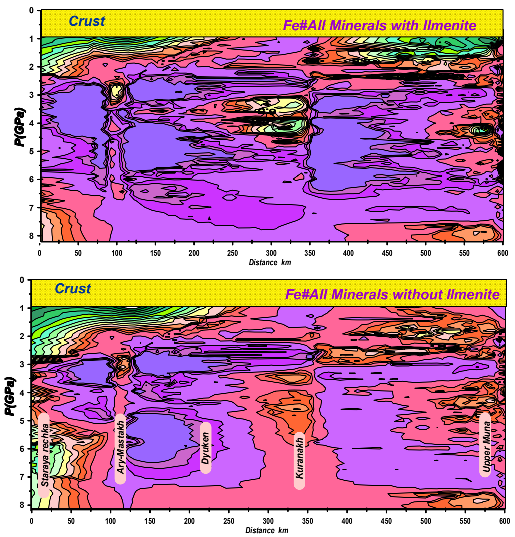

Fig.3

A.,B M antle xenoliths from Zapolyarnaya pipe with visible Cr-diopsides and garnets.
C. Large mantle xenolith from Zapolyarnaya pipe.
D. Segregations of the olivine grains and dunite debris in kimberlites

A.

B.

C.

D.

Compositions of Cr-garnets from Upper Muna (xenolith and concentrate)

A. Zapolyarnaya; B. Novinka;

D. Deimos; Komsomoslkaya - Magnitnaya

Garnets from the Upper Muna kimberlites trace the lower part of the lherzolite field up to 14 wt% Cr_2O_3 in the Cr_2O_3-CaO diagram but most have harzburgitic and dunitic compositions and pyroxenitic types are really scarce.

The most representative and continuous garnet trend for Zapolyarnaya pipe reveals the rarity of pyroxenitic varieties (Fig. 4a). Sub-calcic garnets appear from 1.5 wt % Cr_2O_3 forming three sub-trends parallel to the Cr_2O_3 axis. The enrichment to 1.2 TiO_2 wt. % is more visible in the lower Cr part; the Na_2O elevation to 0.3 wt. % is lower than in other pipes.

In the Novinka pipe, the dunite-harzburgite garnets are restricted to the 5-12 wt % Cr_2O_3 intervals and in the Deimos pipe from 2 to 11 wt % (Fig.4b). The dunitic ones continue the trend to 14 wt% Cr_2O_3. Most of them fall at the upper boundary of the harzburgites field but dunite garnets also appear in the 5-11 wt % Cr_2O_3 interval. Garnets from Komsomolskaya-Magnitnaya and Deimos contain from 2 to 12 wt. % Cr_2O_3. The Ti, Na metasomatism of garnets is more pronounced in Novinka and Komsomolskya-Magnitnaya pipes.

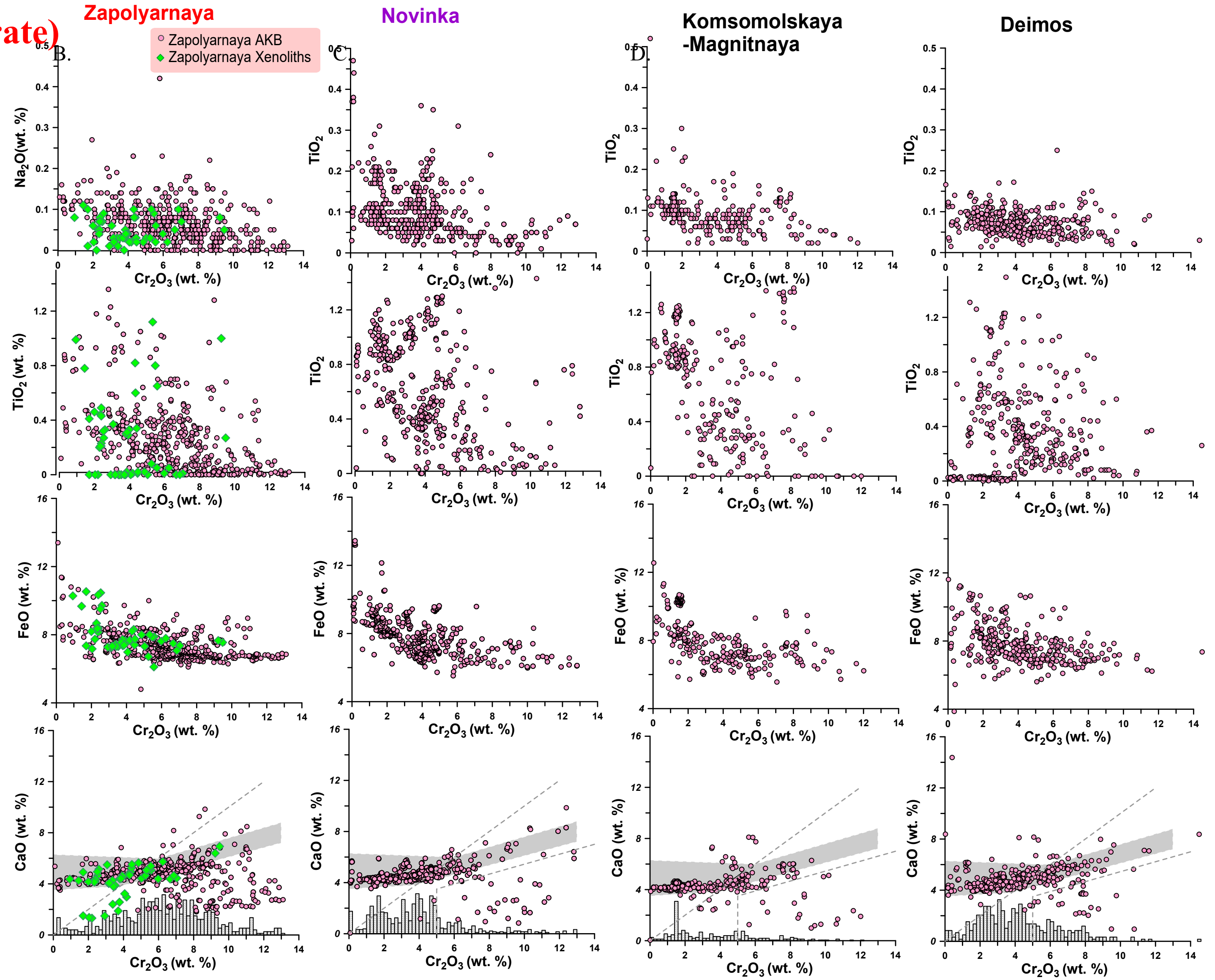

Compositions of Cr-diopsides from Upper Muna field (A) Zapolyarnaya; B. Novinka, Deimos, Komsomoslkaya - Magnitnaya

Clinopyroxenes from the xenoliths of the Zapolyarnaya pipe show a variation in FeO from 1 to 5 wt. % and nearly constant Al_2O_3, close to 1.5-2.5 wt. % (Fig.5a). Only a few Cpx close to omphacites have 6-10% wt. % Al_2O_3 (Fig.5a). The Cpx with 1% wt. % are enriched in Cr_2O_3 to 5 wt% and it wall down to 0.2 at 6 wt. % FeO. In general the pyroxenes enriched in FeO to 3.2-4.5 wt. % are close to those from deformed peridotites. More Fe-rich varieties probably come from the Ilm-bearing associations and intergrowths with ilmenites like those found in Dalnyaya pipe (Ashchepkov et al., 2017c). But TiO_2 content is low (to 0.4 wt. %) increasing for Fe-rich varieties, tending to omphacitic Cpx or Al-augites. Cpx are relatively common (Fig.5b) in the concentrate from all other Upper Muna pipes. In general they show similar trends as for Zapolayrnaya pipe but variations in TiO2 and Al2O3 are wider. Novinka Cpx show much wider variations in Al2O3 up to 6 wt. % in the Fe-poor part of the trend. TiO2 increases together with FeO to 0.5 wt. %. Cpx from Deimos pipe show strongest Cr-Al variations, probably due to hybrid metasomatism and the presence of eclogite types of Cpx.

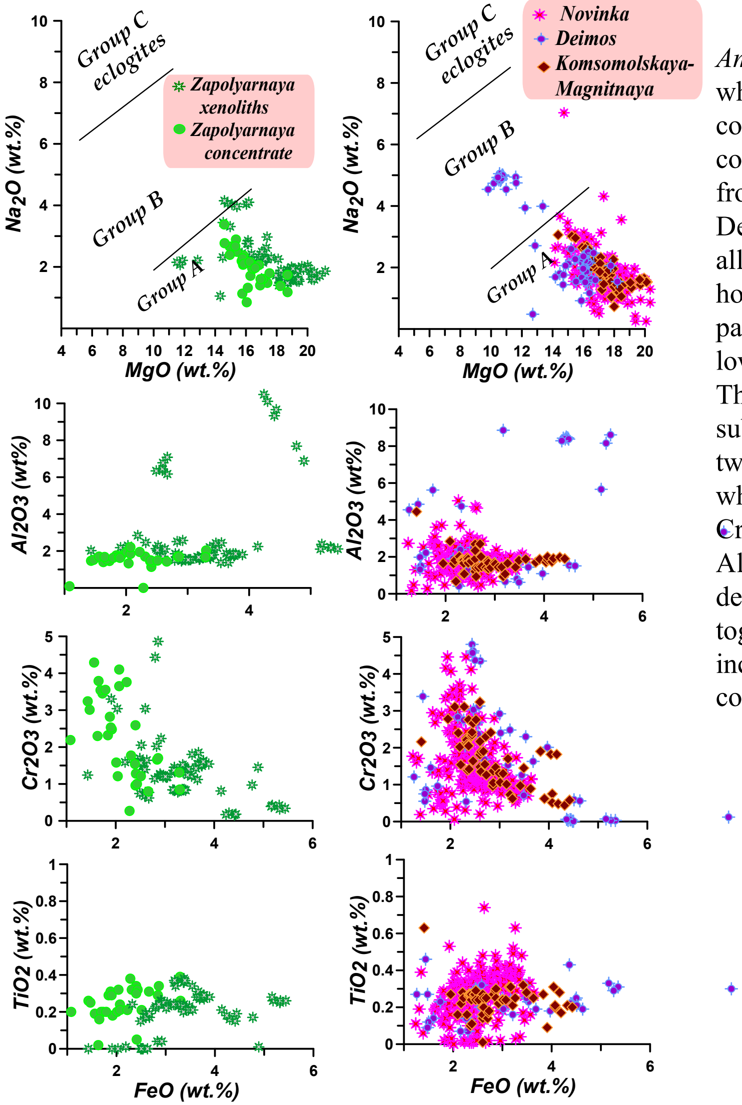

Compositions of amphiboles from Daldyn and Alakite fields and Upper Muna field,

Amphiboles A. which are more common in the concentrate from the Deimos pipe are all Cr-Ca hornblendes and pargasites with low Ti contents. They may be subdivided into two groups where K_2O, Cr_2O_3 and Al_2O_3 slightly decrease together with increasing FeO content

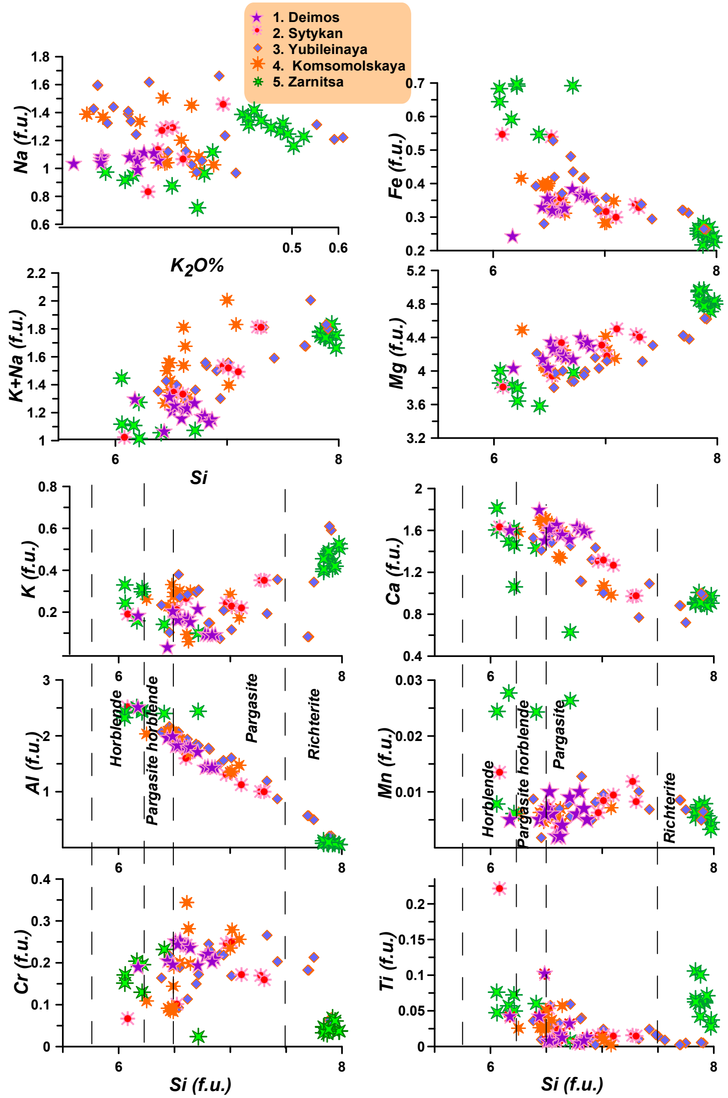

Compositions of chromes from Upper Muna field (A) Zapolyarnaya; B. Novinka; Deimos, Komsomolskaya - Magnitnaya

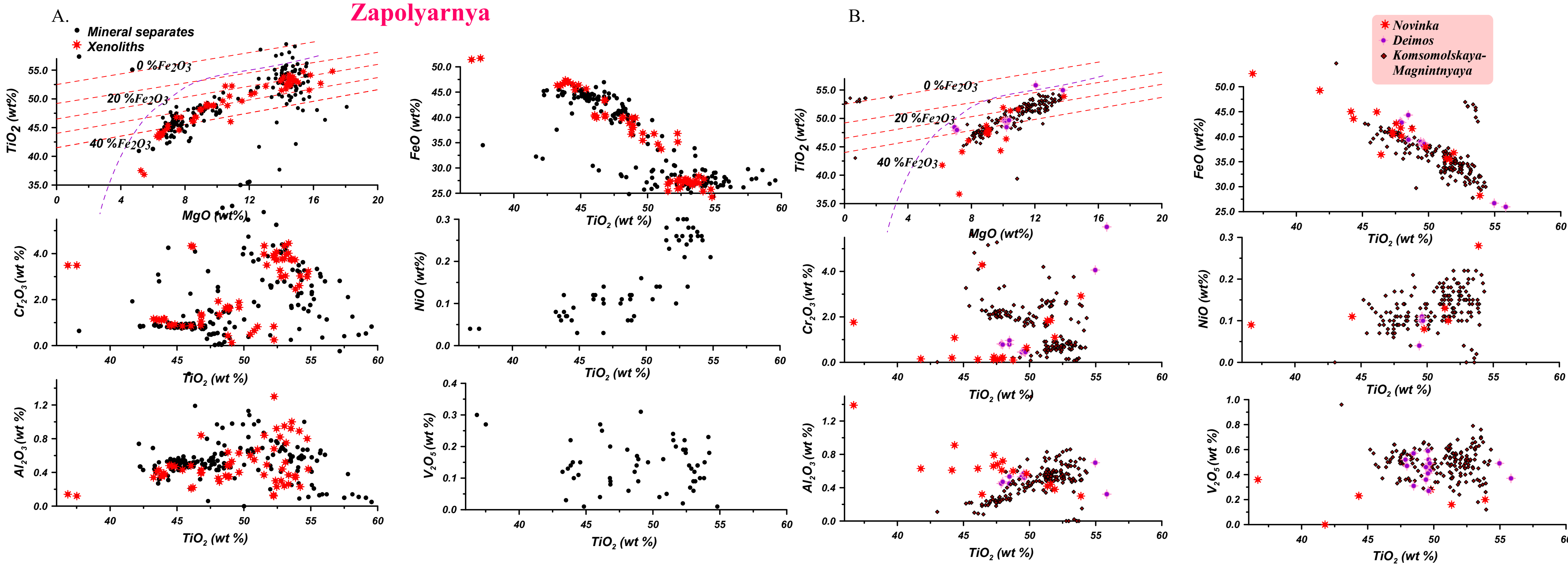

Ilmenites from Zapolyarnaya (Fig.6A) show wide variations in Cr_2O_3 which show the trend of enrichment to 6 wt. % in TiO_2 interval varying from 56 to 50 wt.% reflecting the increasing contamination in peridotite material (Al_2O_3 and NiO are also high), while ilmenites of the middle and low-TiO_2 part are less contaminated. In Deimos, ilmenites are rather abundant and show variations typical for those from kimberlites of Alakit and Daldyn region with nearly linear FeO- MgO- TiO_2 relations (Fig.6B) (Ashchepkov et al., 2014, 2017b), usually considered to be a fractionation trend. Mg varieties are relatively widespread compared to Zapolayrnaya. The Ti-Mg-Cr-rich varieties are higher in NiO and other components and correspond to metasomatites. The more differentiated and low-TiO_2 ilmenites split into two branches with different Cr_2O_3 contents. The Al_2O_3 content decreases in three linear trends from 54 to 52 wt.% TiO_2, possibly showing three groups of melt reactions with garnets.

A.

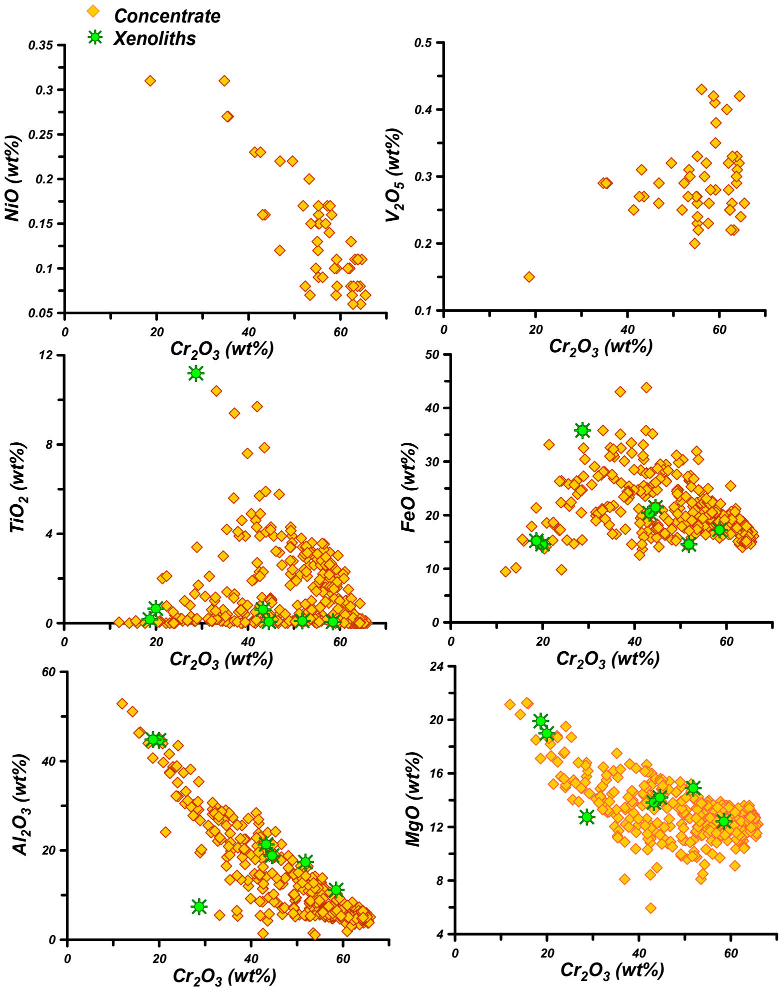

B.

Compositions of chromes from Upper Muna field (A) Zapolyarnaya; B.Novinka;Deimos, Komsomolskaya - Magnitnaya

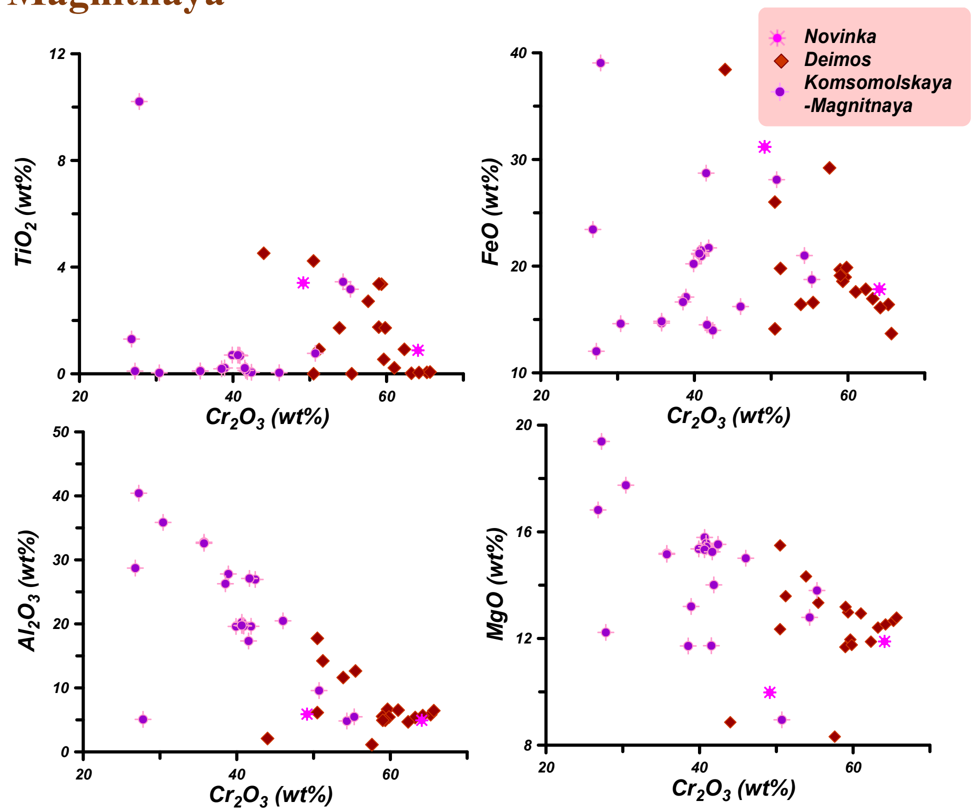

Chromites from Zapolyarnaya show a long trend from 68 to 10 wt.% Cr_2O_3 (fig.7A). The most Cr-rich varieties (65-61 wt.%), typical for diamond inclusions (Logvinova et al., 2005; Sobolev et al., 2004), are mainly low-Ti but those lower in Cr belong to two trends. The ulvospinel branch shows enrichment in TiO_2 up to 11 wt. %, together with an increase in NiO content with a general decrease in V_2O_5 from 0.5 to 0 wt. %, showing that ulvospinels were more oxidized. The other pipes have similar variations but with far fewer analyses

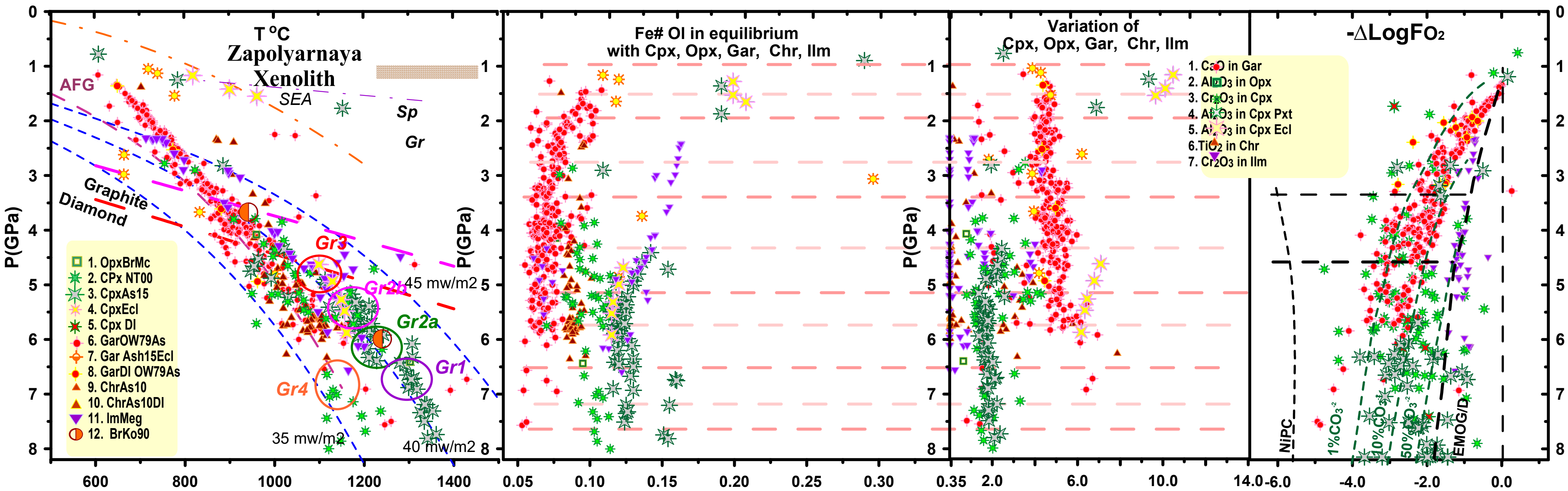

PTXfO$_2$ diagram for the minerals from deep seated xenoliths from Zapolyarnaya pipe. It addition added some xenocryst from essentially "dunite veins"

Signs: 1. Opx: T^{o}C (Brey and Kohler, 1990)-P(GPa)(McGregor, 1974). 2.. Cpx: T^{o}C- (Nimis and Taylor, 2000) P(GPa) - Ashchepkov et al., 2017(forCr - diopsides);3.The same for Ferich Cr -diopsides s. 4.The same for eclogites and and pyroxenite)Gar: 6..T^{o}C (O'Neill and Wood, 1979) -P(GPa) (Ashchepkov et al ., 2017), 7.The same for eclogites; 8.The same for diamond inclusions. Chromite 9.T^{o}C (O'Neill and Well, 1987)-P(GPa) (Ashchepkov et al., 2010); 10. The same for diamond inclusions. 11. Ilmenite megacrysts T^{o}C (Taylor et al., 1998)- P(GPa) (Ashchepkov et al., 2010); 12. T^{o}C-P(GPa) (Brey and Kohler, 1990). The compositions of the diamond inclusions is taken from (Bulanova, 2004).

The field for P-FO2 diagrams after Stagno et al. (2013). The horizontal dashed line at 3.5 and 4.5 GPa corresponds to the Graphite-Diamond boundary at 35 and 40 mWm-2 respectively.

A. **PTXfO_2 diagram for the concentrate from A. Zapolyarnaya pipe. B. The same for Deimos pipe**

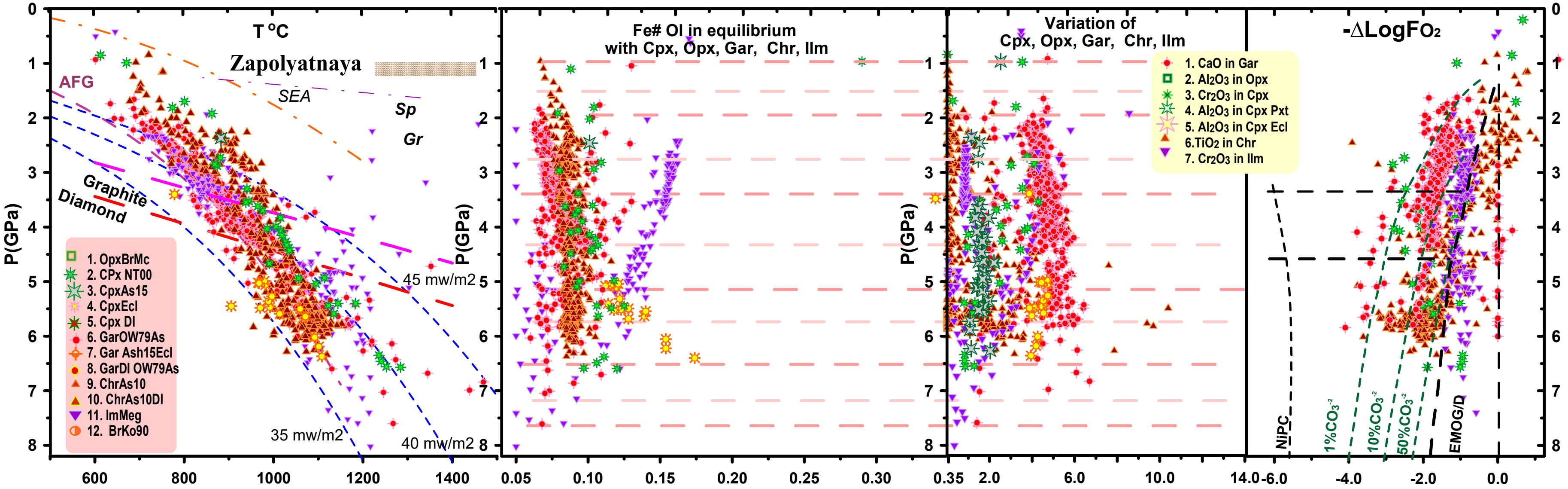

B.

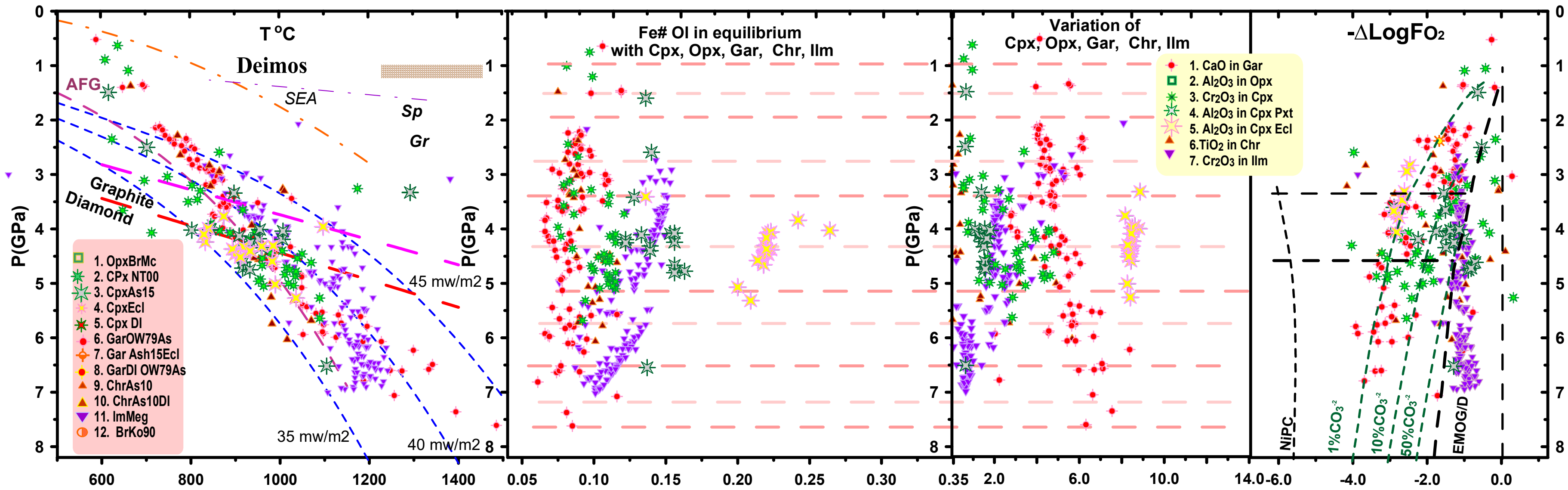

The PT estimates and geochemistry minerals for 50 xenoliths from Zapolyarnaya pipe were obtained for the first time. All the PT reconstructions were made using monomineral versions of thermometers (Ashchepkov 2010-2017) for garnet, clinopyroxene, orthopyroxene, chromite, ilmenite and amphibole compositions.

The garnet geotherm (Fig.9) is relatively high temperature and extends to 8 GPa splitting into lower-T (35 mWm^{-2}) and high-T (45 mWm^{-2}) branches. In the upper part it becomes sub-adiabatic, crossing conductive geotherms. The garnet trend became more Fe-rich in the upper sub-cratonic lithospheric mantle (SCLM). The alternative themobarometer (Griffin et al., 1989; Ryan et al., 1996) used by Griffin et al (1999) always locates all the PT points near the diamond-graphite boundary except for several sub-Ca garnets. Commonly they also project Ni temperatures onto the 40 mWm^{-2} geotherm (Batumike et al., 2009).

Most Cpx from the xenoliths are refertilized types like those from deformed or porphyroclastic peridotites from Udachnaya (Ashchepkov et al., 2014). They also give a high-T geotherm tracing a convective branch (40 mWm^{-2}) with an inflection at 6 GPa. A low-T branch also exists. The P- Fe# trend for Cpx splits. The middle values are close in Fe#Ol to the ilmenite trend, whereas the lower Fe# values are close to those of the common peridotitic garnets and the higher one is pyroxenitic. Some eclogitic Cpx (Cr-bearing) are found in the middle part of the section tracing the Ilm trend. They are Al-Na-rich and most probably are cumulates from hybrid melts that reacted with primary eclogites The highly Fe-rich pyroxenitic Cpx correspond to the Moho boundary.

In the deeper part of the SCLM, the Cpx are essentially more oxidized and closer to values of ilmenites. In the upper part of SCLM the products of fertilization refers to more reduced conditions close to garnet trend the Cr-diopsides refer to the oxidation state of garnet (McCammon et al., 2001) trend (10-20% CO_3^{-2} in melt) (Stagno et al., 2013).

The $PTXfO_2$ diagram for Zapolyarnaya based on KIM from concentrate (Fig.10A) shows nearly the same geotherm for garnets. Mantle section is layered according to garnets showing several (at least 6) Ca-rich jets in P(GPa)-CaO trend. At the same sub-Ca garnets found from 2 to 8 GPa in mantle section are more frequent and probably refer to the continous dunite channels. The Cpx that show a common peridotitic signature represent the range from the lithosphere base to 1.5 GPa. The ilmenites of Fe-Ti type give a rather complex trend from the lithosphere base to 2.5 GPa. But there is also a separate Mg-rich trend corresponding to the dunitic values (Fe#Ol=0.07) is tracing the entire lithosphere thickness. Cr-rich (to 5 wt %) ilmenites found from 6 to 3 GPa suggest intense protokimberlite metasomatism in the mantle column. Chromite PT values give a rather wide geotherm close to those determined for garnets. Ti-rich varieties are more frequent in the lower part of the SCLM.

The nearby Deimos pipe reveals rather different thermal conditions having a lower (35 mWm^{-2}) geotherm at 6 GPa and inflection and convective heating branch (to 45 mWm^{-2}) in lower mantle part to 8 GPa. There are three levels at 3.5, 4.8 and 5.5 GPa with the increasing Fe values. The amount of dunitic garnets is higher in the middle and lower parts of the SCLM but the pyroxenitic trend in lower part from 4 GPa is more pronounced. There are at least three types of Cr-diopsides –the first is in the middle part, close in Fe#Ol to Cr-garnets from peridotites (lherzolites), the 2nd trend is intermediate between ilmenitic and peridotitic trends and the third is close to the ilmenite fractionation trend. Typical eclogitic Cpx form the small trend from 5 to 3.5 GPa. The ilmenite trend also has three branches: the first is low-Cr at 7-6.5 GPa; the second has moderate Cr from 5 to 3.5 GPa and the third is Cr-rich to 2 GPa related to the Amph-Phl metasomatites.

In the mantle structure beneath Novinka, the garnet geotherm is similar to those from the previous pipes but at slightly lower temperatures. It is divided into several (4 large) sharp intervals with positive inclinations of the P-Fe trends. Garnets also show a depletion trend starting from 2 to 7.5 GPa and at the lithosphere base at ~7 GPa the garnet trend in P-CaO plot splits into pyroxenitic and dunitic branches. This mantle column contains more fertile material than that beneath Zapolyarnaya and Deimos. Cr-diopsides vary in Mg# from 0.93 to 0.84, showing three definite trends in P-Fe#. The first is for common lherzolites. The second is close to the ilmenite trend. And there is a more Fe-rich branch that probably appeared after the reactions with eclogites when eclogites are melting and transforms to pyroxenites (Rosenthal et al., 2018).

The $PTXfO_2$ diagram for the Komsomolskaya-Magnitnaya pipe is similar to those determined for Novinka. But the abundance of pyroxenes is lower and they are mostly located in the 3.0-6.5 GPa interval. The pyroxenite branch exists only in the deeper part of the mantle column at 7-5 GPa and corresponds to the Ilm trend.

A.

PTXfO$_2$ diagram for the concentrate from A. Novinnkapipe. B. The same for Komsomolskyaya Magnitnaya pipe

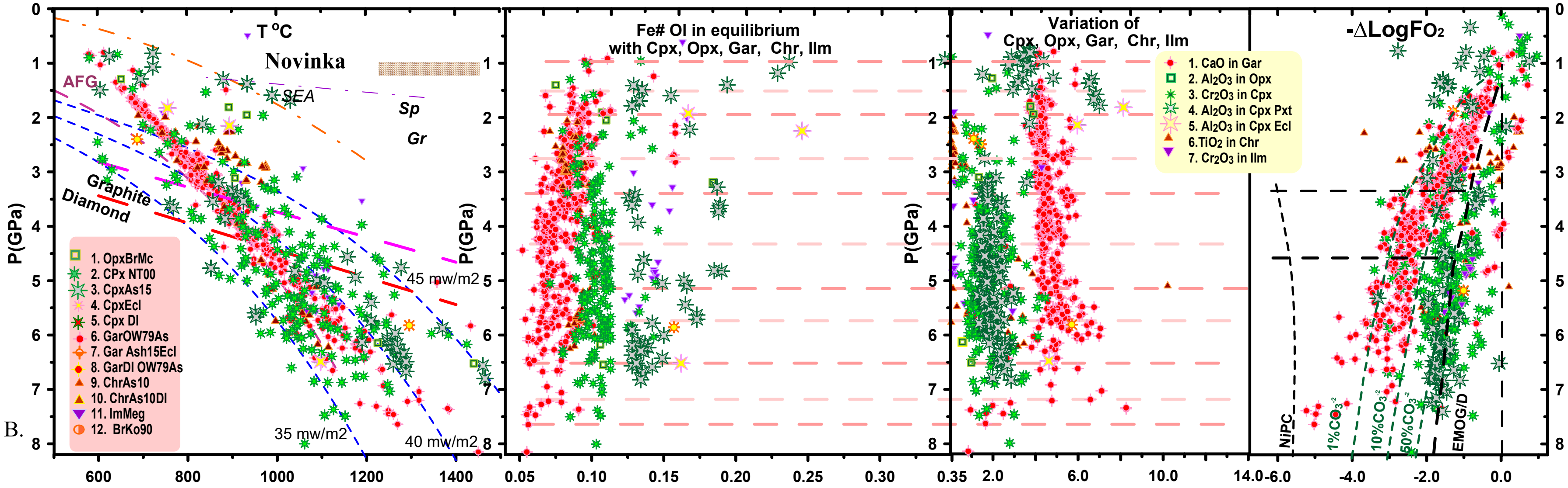

B.

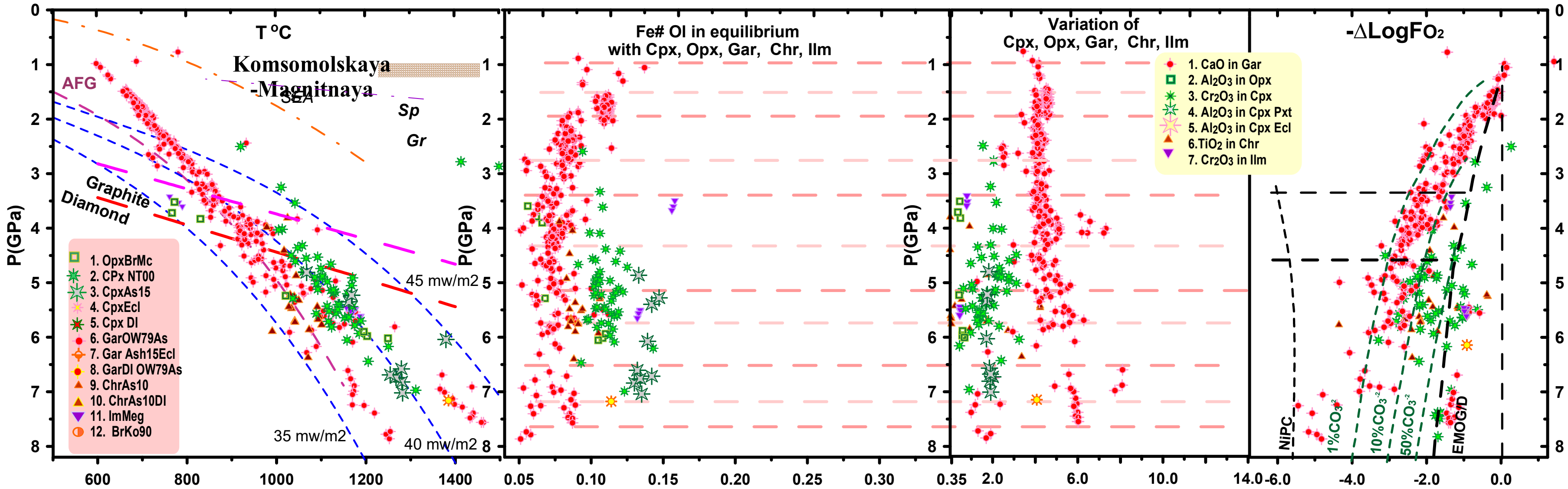

Cr garnets from mantle xenolith Zapolyarnaya pipe

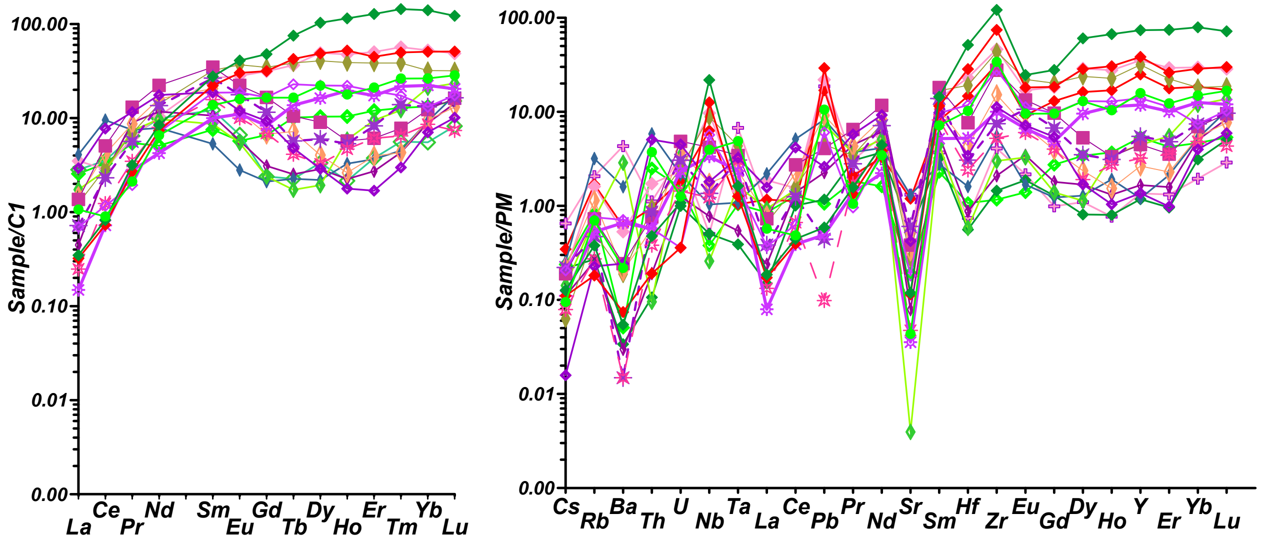

REE and TRE spider diagrams for the high-Cr garnets from mantle xenoliths of Zapolyarnaya pipe. Normalization to chondrite C1 (Evensen et al., 1978) and primitive mantle (McDonough and Sun 1995).

Cr garnets from Zapolyarnaya pipe concentrate

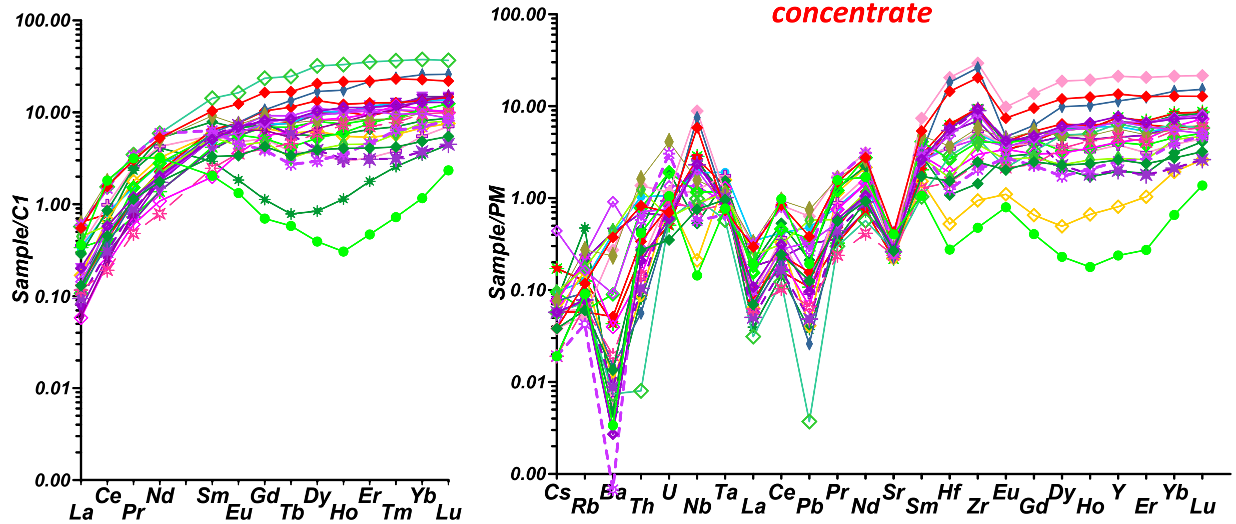

REE and TRE spider diagrams for the high-Cr garnets from concentrates ABK of Zapolyarnaya pipe.

Trace element geochemistry

REE patterns for garnets from the Zapolyarnaya xenoliths show S-type for ~50 % of the analyzed population. These patterns show the minima from Er to Tb and they rarely reveal pyroxenitic slightly concave-up patterns (Fig.12). They have HFSE enrichment (mainly Zr>Hf and asynchronous Nb, Ta), and even slightly elevated LILE. Those with high REE contents have significantly higher Zr, Nb, Th peaks, suggesting hydrous Phl-bearing metasomatism (Griffin et al., 2002) accompanying (and prior to) intrusion of protokimberlite magmas. Garnets from concentrate also contain similar dunitic garnets and S-type patterns (Burgess & Harte, 2004) (Fig.13) but they show lower HFSE and LILE abundances. Two pyroxenitic garnets show joint Zr-Hf peaks. Common lherzolitic-harzburgitic garnet varieties practically all have more elevated Ta and fluctuating Nb contents.

The Cpx reveals division into 4 groups. Three of them have similar asymmetric bell-like REE patterns like those from megacrysts from the Dalnyaya pipe (Ashchepkov et al., 2017c) with increasing REE level (100 to 10/C1) and La/Ybn. Pyroxenes from the first group with lower trace element contents have semi-round trace element patterns (Gd/Yb)n ~ 5-7 with minima in Zr, Hf, Pb and local small peaks of Sr, Nb, Th. Pyroxenes from group 2 are more inclined and have in general higher trace element patterns without Sr peaks. Pyroxenes from the third group have much higher trace element contents and show high Zr, Hf and peaks in Nb, Th and sometimes in Pb. The fourth group of Cpx has the highest inclination of REE (La/Yb)n>20 and a flatter part from Sm to La. They have negative HFSE but elevated Rb, Ba Th, U ~10/C1 but lower than La.

Cpx from the concentrate of Zapolayrnaya pipe show slightly different but also inclined REE patterns have slightly concave up REE pattern from La to Nd and then demonstrate (Gd/Yb)n ~10. The Zr-Hf and Ta-Nb minima are found in two Cpx with lower REE contents. The others have more elevated HFSE at the same level as REE. Ba and Th peaks are found for more enriched varieties.

One amphibole shows a straighter inclined REE pattern and spider-diagram with elevated HFSE and peaks in Rb, Ba.

Garnets from Novinka pipe concentrates have fewer dunitic varieties. They show more asymmetric S-type patterns with peaks in Pr-Nd and variations in HFSE. The HFSE peaks are typical for the REE-enriched varieties and sometimes they reveal U and Th peaks, probably suggesting subduction-related features (Manning, 2004). The common garnets with nearly flat REE part from Sm to Lu or slightly inclined show an increase in the HFSE: Zr>Hf and Nb>Ta.

The Zr peaks suggest an origin for the Cpx which requiures much more hydrous metasomatic conditions. In general, this reflects polybaric interaction of the evolving proto-kimberlite melt with the depleted peridotite mantle. The focus of the interaction in Upper Muna was beneath the Zapolyarnaya pipe.

Clinopyroxenes from Novinka pipe from Gr1 to Gr3 demonstrate spreading fan-like in left part REE patterns when difference for the left elements in REE diagram became higher starting from Sm to La. Some more differences they reveal in the TRE spider diagrams.

The first prevailing group has moderately inclined REE patterns (La/Ybn ~10-15 with a gentle hump at Nd-Pr (La/Smn <1). Those with lower REE concentrations are also depleted in general in the left part of the spider diagram but the others demonstrate temperate incompatible element (IE) enrichment and slightly elevated LILE. Cpx from groups 1-2 have small depletions of Zr< Hf as well Ta and Nb. But Cpx from Gr3 have Ta minima. The 3d group shows the most strongly inclined REE patterns with an inflection at Nd and a flat left part of the REE diagram. But these Cpx have in general very low incompatible elements except for one which has incompatible elements at average level and slightly elevated LILE.

REE and TRE spider diagrams for the –Cr- diopsides from mantle xenoliths of Zapolyarnaya pipe.

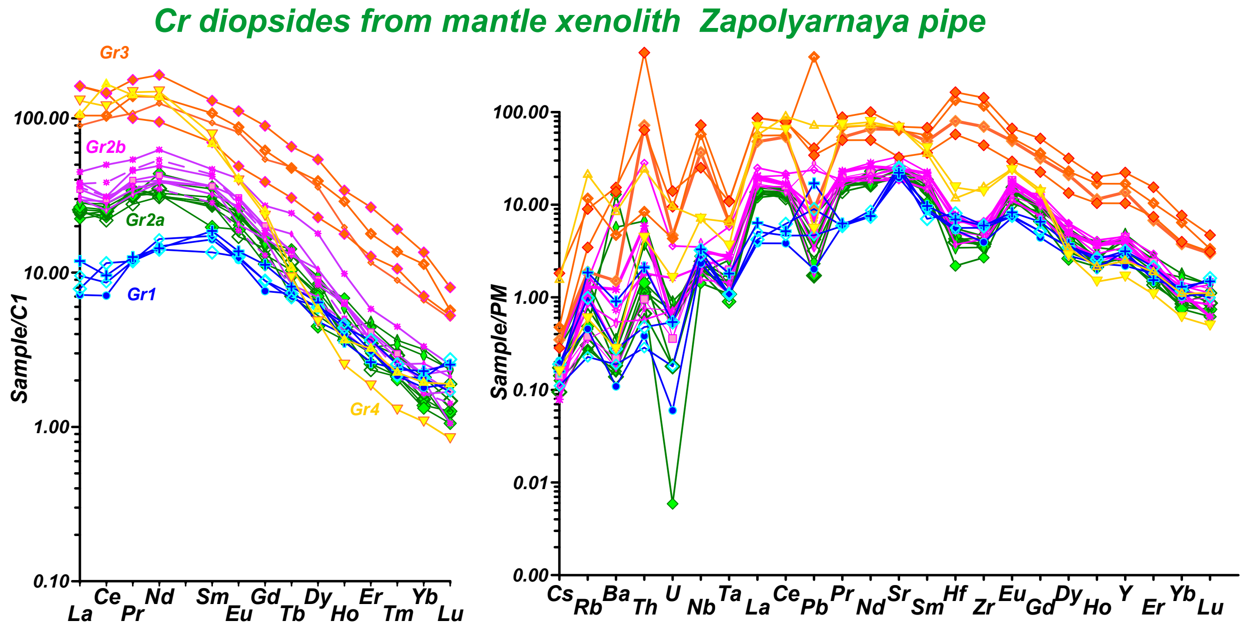

REE and TRE spider diagrams for the –Cr- diopsides from mantle xenoliths of Zapolyarnaya pipe.

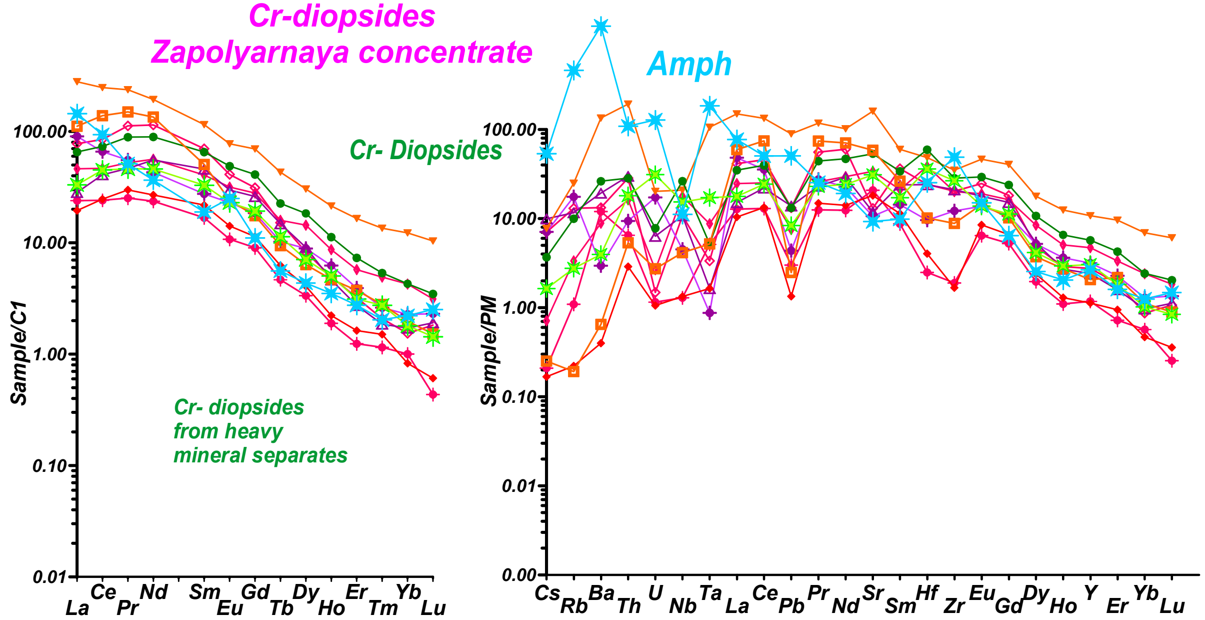

REE and TRE spider diagrams for the high-Cr garnets from concentrates ABK of Novinka pipe.

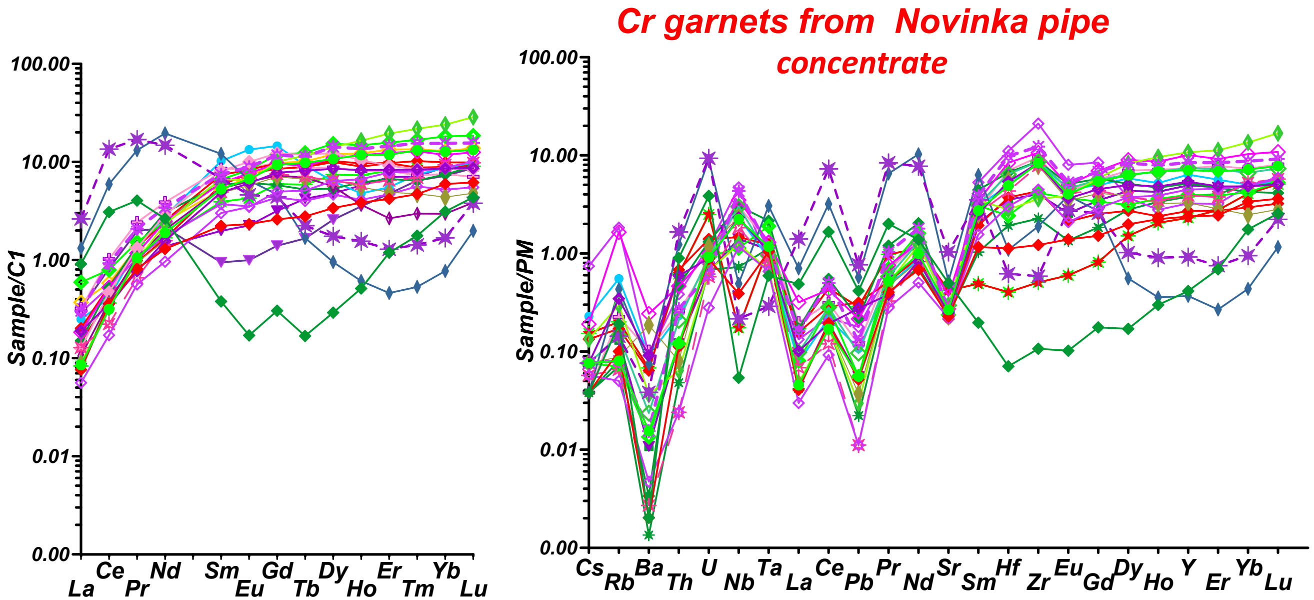

REE and TRE spider diagrams for the –Cr- diopsides from concentrates of Novinka pipe.

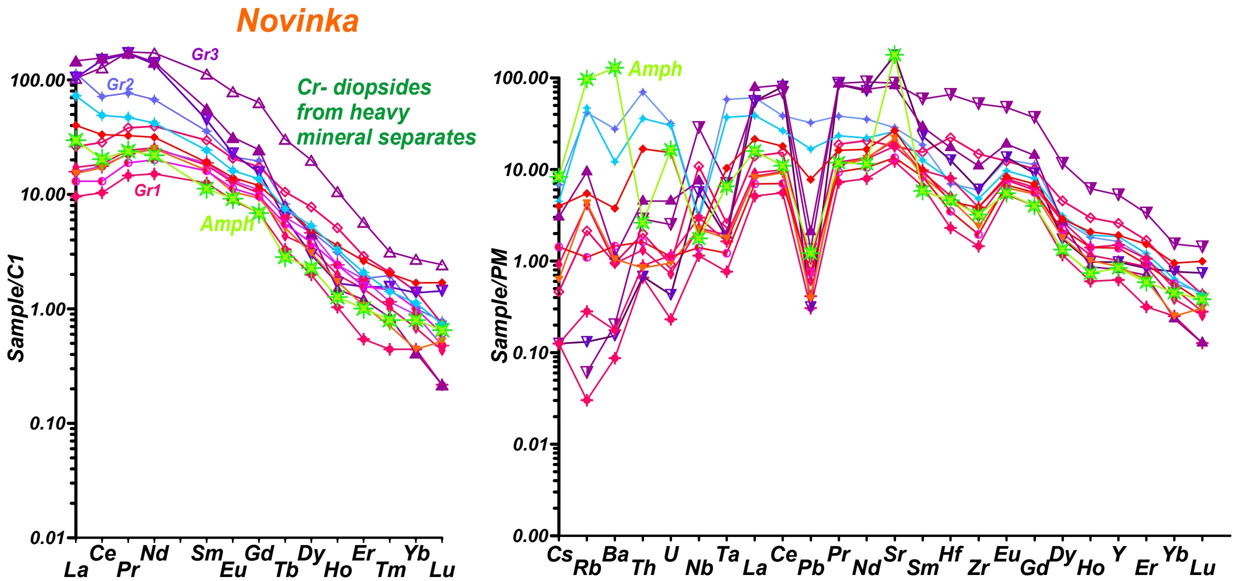

Melts parental for calulated with Kd (Hart, Dunn, 1993)
Cr diopsides from mantle xenolith Zapolyarnaya pipe

A.

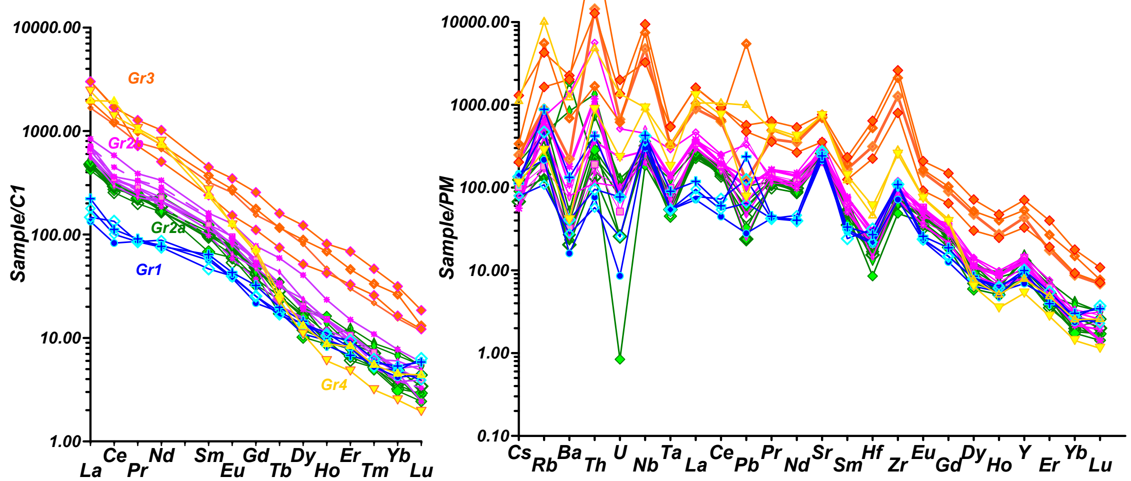

B.

Melts calculated with the KD (Green et al. ,2000)
parentalfor the Cr garnets from mantle xenolith Zapolyarnaya pipe

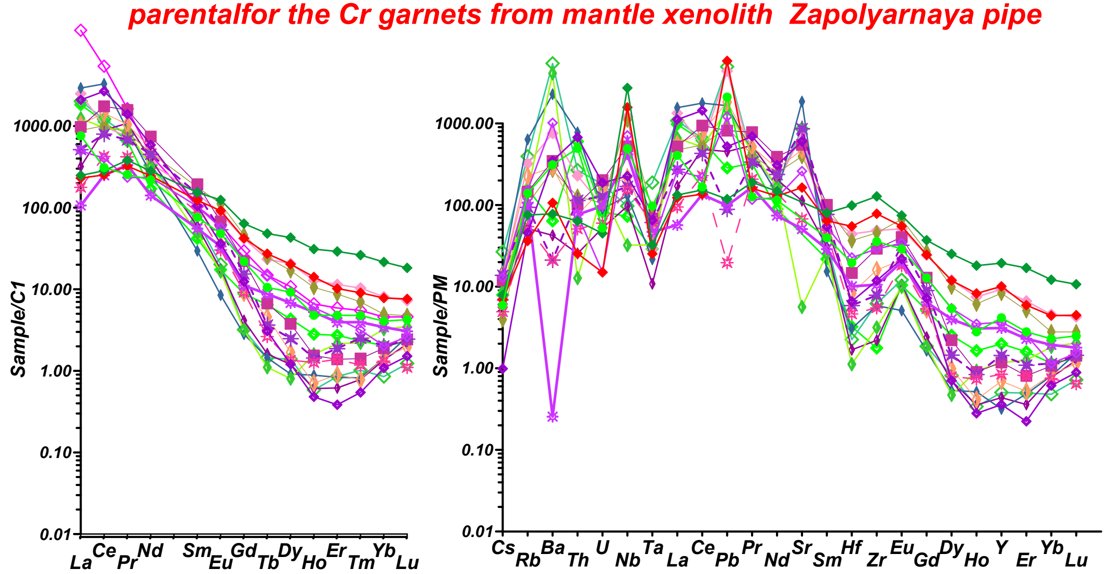

Metasomatism and geochemistry

From the geochemistry it is clear that there are two types of metasomatism. The first is connected with the protokimberlite melts which produces the stepped increase of REE and TRE and follow the protokimberlite differentiation and also partial melting of peridotites. In first two groups the influence of partial melts is not so clear but for the Gr2b the incompatible elements slightly grow up. For the Gr 3 and Gr 4 groups the influence of metasomatic components became clearer. The reconstructed melts with the KD (Hart & Dunn, 1993) with the addition of KDs from (Klemme et al., 1995; Hauri et al., 1994) (Fig17) show that the jagged spider-diagram which may be derived from essentially oxidized carbonatitic melts which party lost HFSE. But the elevated amounts of such components LILE, Sr, Th , Rb, Nb, Y, U may also suggest contamination in some subducted material which could also incorporate continental sediments (Manning, 2008; Xu et al., 2019) and has the strong Zr peak. Further enrichment causes the appearance of the strong peaks and also elevation in Rb and all LILE.

The parental melts for the garnet from the xenoliths (Kd after Green et al., 2000) (Fig. 18B) essentially differ. Even common garnets have different inclination of REE patterns and mostly slightly concave and the dunitic garnets reveal the higher inclination with the hump at Ce -Pr and depressions from Gd to Yb. The observed peaks in Rb, Ba, Th, Nb, Pb and Zr are closer to subduction type. Thus the garnets and clinopyroxenes in xenoliths are in total disequilibrium.

The key question about the metasomatism is the behavior of the HFSE and mostly Zr which became higher with the REE level. As is clear from all the magmatic processes, Zr is an indicator of high activity of H2O in melts. Enrichment of the later Cpx in Zr and LILE could be result of two alternative processes. The first is the differentiation or mixed carbonate – H2O-bearing alkaline melts which are found sometimes as melt inclusions (Golovin et al., 2018). The other possibility is the admixture of partial melts in peridotites after melting of Phl-bearing metasomatites which increase the LILE and LREE. The rise of Th and Nb may be explained by the original subduction material containing rutiles and possibly some rare minerals like apatites, even monazite or zircons and perovskites. Rutile is effective at decoupling Nb and Ta (Klemme et al., 2005) and possibly that ancient subduction factory still determine the geochemistry of the Upper Muna mantle silicate minerals. Enriched in REE garnets most frequently reveal the enrichment in HFSE and in Zr especially suggesting the reactios wit the differentiated H2O bearing melts.

One more specific thing is the differences of the dunitic garnets from Novinka which are very LREE enriched and have U peaks. Garnets from concentrate and xenoliths from Zapolyarnaya pipe also have U and Ta peaks, probably a sign of ancient subduction-related fluids.

The patterns of Cpx from the Novinka pipe are more controversial. The most REE-rich compositions Gr3have very low IE and slightly lower in REE group 2 have the highest IE part including REE. It means that the Gr2 was crystallized from the melt mixed between the peridotite metasomatites and protokimberlites. And Cpx from Gr3 include pure derivates from protokimberlites and contaminated varieties.

Relations of the dunites, diamonds and protokimberlite metasomatism.

The abundance of depleted peridotite and subcalcic garnets (G9-10) associations is rather high for the perspective of diamond production (Stachel & Harris, 2008). Moreover the dunites served as melt conduits (Akizawa et al., 2016, Kelemen et al., 1998), although the protokimberlitic melt chose Zapolyarnaya pipe as the main melt conduit.

The mineralogical features as well the structure of the mantle columns of the Upper Muna mantle slightly differ from those of the other regions of Siberian platform. Widespread enriched Cr-diopsides that are found in diamond inclusions are not very common for the Daldyn and even Alakit region. The rather low abundance of ilmenites is more similar to the Nakyn field than for the central region. The structure of the mantle columns shows also the abundance of the pyroxenite material in the lower horizons of the mantle which is more typical for the mantle column beneath the continental type of mantle.

Heating of the lower SCLM is more pronounced for the Zapolyarnaya pipe and it is suggested to be more prospective for large good quality diamonds because many large pipes like Premier (Korolev et al., 2018), Orapa (Aulbach et al., 2017), Zarnitsa, Mir, Udachnaya with very heated lithosphere base and deep roots. And thus the large diamonds that are found in this pipe (Fig.2C) may be referred to the type II diamonds megacrystic diamonds according to classification of Moore et al (2009). The appearance of the lithosphere base in turn is formed due to reaction of the oxidized melts with the lithosphere and has a minimum in mechanical strength at 6. GPa (Karato, 2010). In such weakened and rather reduced conditions buffered by peridotites, the growth of diamonds is possible.

The other types of diamonds may be also of slightly rounded form may be products of crystallization of some smaller portions of alkaline carbonatitic melts partly reduced on the mantle peridotites due to contamination which spread in the mantle column. According to experimental data, the presence of H_2O causes rapid diamond crystallization (Pal'yanov et al., 2002) and the complex shapes of the crystallized diamonds (Palyanov et al., 2015). Moreover they demonstrated that for diamond crystallization at 7.5- 6.3 GPa at the base of the lithosphere, the temperatures should be 1450-1570oC (Palyanov et al., 2018) which just corresponds to the conditions of the protokimberlites at the LAB, and conditions determined for the SCLM beneath the Zapolyarnaya pipe. Presence of the Phl in diamonds (Sobolev et al., 2009) supports this idea. Though the diamonds of course could have different time of origin in different conditions (Sobolev, 1977) but now more information is being published about the formation of diamonds close to protokimberlite processes.

The parental melts for Cpx are similar to protokimberlites in REE elements, but they essentially mixed with metasomatic material. This is accompanied by increasing oxidation of Cr in Cr-diopsides and increase of all incompatible elements and general reduction in fO_2 during rising and reacting of protokimberlite melt with the mantle.

Conclusions

1. The Upper Muna field includes four diamondiferous pipes which contain deep material typical for the basement of the continental keel, very rich in the depleted varieties and subjected to the subduction-related Phl metasomatism in ancient time
2. The geochemical features with Zr and Th peaks and enrichment in LILE of peridotite minerals show rather enriched continental or metasomatic signatures.
3. Multistage processes of melt percolation recorded at the PT paths in mantle columns suggest a rather permeable lithospheric mantle structure.
4. The largest diamonds as well as other good quality diamonds may result from the crystallization of protokimberlite melts highly contaminated in peridotites or mixed with partial melts from metasomatized peridotites.
5. The structure and mineralogical features and their trace element signatures may be rather prospective for diamond exploration.

Acknowledgements.

Supported by RFBR grants 19-05-00788, 16-05-00860 and joint research projects IGM SB RAS and ALROSA Stock company 77-2, 65-03, 02-05.Work was done on state assignment of IGM SB RAS, governmental assignment in terms of Project IX.129.1.4.

Thank you for attention!!!!